

Integrated Slotted SIW Oscillator-Antenna Based on the TE_{210} Mode with High Spectral Purity

Abdelmounim Sellidj^{1,*}, Tarek Djerafi², Said Gaoua¹, and Mustapha C. E. Yagoub³

¹LINS Laboratory, University of Science and Technology Houari Boumediene USTHB, Bab Ezzouar 16111, Algeria

²Institut National de la Recherche Scientifique, Université du Québec, Montreal, QC H5A 1K6, Canada

³School of Electrical Engineering and Computer Science, University of Ottawa, Ottawa, ON K1N 6N5, Canada

ABSTRACT: In this work, a Substrate-Integrated Waveguide (SIW) cavity-based positive-feedback oscillator integrated with a slot antenna on a single substrate was designed. The proposed design incorporates a radiating element, an oscillator tank, and a coupling structure within the same cavity, thereby eliminating external interconnections and significantly enhancing overall efficiency. By employing the TE_{210} mode instead of TE_{110} , the design exploits a field node to minimize the parasitic loading effects of the oscillator coupling probe on the antenna radiation. This approach simultaneously enhances the cavity's quality factor Q and preserves the spectral purity of the integrated SIW antenna-oscillator, all this without affecting the antenna radiation. The SIW cavity achieves a measured quality factor Q of 250, ensuring high spectral selectivity at the 10 GHz resonant frequency. The oscillator exhibits low phase noise of -131 dBc/Hz at a 1 MHz offset, along with exceptional suppression of harmonics, including the total suppression of the third harmonic, while the slot antenna achieves a gain of 6 dBi. This fully integrated architecture delivers performance equivalent to discrete implementations while offering a compact footprint and eliminating insertion losses between the antenna and the oscillator.

1. INTRODUCTION

Antennas and oscillators are fundamental components in modern radio frequency (RF) transceiver front-end systems. Integrating these two functions into a single component significantly reduces RF front-end complexity and enhances overall system compactness. Substrate Integrated Waveguide (SIW) technology, due to its ability to realize high-quality-factor (high- Q) resonant cavities, is particularly beneficial for developing integrated cavity antennas and oscillators. SIW's planar structure also facilitates integration with other RF components, offering cost-effective and scalable solutions suitable for compact, power-efficient systems [1–8]. The recent literature presents various approaches to SIW-based cavity antennas [7], oscillators, and active antenna oscillators [4, 6, 9–13]. For instance, a simple SIW-based self-diplexing antenna employing two microstrip feed lines and dual transverse slots was proposed in [7] to achieve high port isolation, independent frequency tuning, and efficient dual-band radiation. A dual-frequency concurrent oscillation was demonstrated through a self-duplexing SIW structure [4]. A filtering rat-race coupler provided frequency stabilization, impedance matching, and power-splitting functionalities in an oscillator configuration [5]. Frequency-tunable oscillation was also achieved using a varactor diode within an X-band cavity-backed active antenna oscillator [6]. Additional examples highlight innovative design methods: a high EIRP (Effective Isotropic Radiated Power) self-oscillating circularly polarized antenna utilized a composite resonator and artificial magnetic conductor to enhance radiated power [9]; a

capacitively coupled region was introduced to improve bandwidth and radiated power in a miniaturized wideband active antenna [10]; harmonic suppression was achieved using metamaterial resonators and ground radiation techniques [11]; differential symmetry was in cross-coupled planar antennas driven by bipolar transistors demonstrated low phase noise and effective harmonic suppression [12]; and an integrated active switching circuit allowed concurrent dual-band oscillation and pulse radiation [13]. These works illustrate the clear advantage of integrating the antenna and oscillator functionalities. Those designs use negative feedback to integrate the antenna with the resonator. In contrast, the use of positive feedback can selectively enhance resonance performance, resulting in sharper frequency peaks, reduced phase noise, and improved frequency stability. In addition, it can be harnessed to improve the spectral purity and precision of RF and microwave sources [14–16].

Conventional integrated oscillators often use negative feedback, which relies on generating negative resistance at a single port and suffers from high phase noise and frequency instability [14, 16]. To overcome these challenges, this paper proposes a unified architecture utilizing the TE_{210} mode in a positive feedback configuration to achieve high Q and superior phase noise.

The primary contribution of this circuit lies in its independent and adjustable coupling control through a cavity probe (port 2 in Figure 1), which does not interfere with the excitation cavity mode. Furthermore, it features an integration of resonator and radiator with reduced mode perturbation, as the radiation slot is positioned at a field node of the TE_{210} cavity mode, where the

* Corresponding author: Abdelmounim Sellidj (asellidj1@usthb.dz).

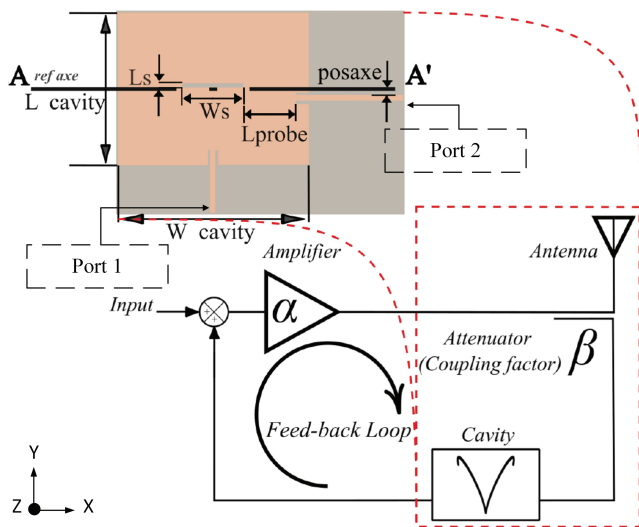


FIGURE 1. Oscillator of proposed architecture with merged coupler/antenna/cavity.

electric field is at its minimum, thereby ensuring minimal field perturbation.

In this work, a novel slot-antenna cavity positive-feedback oscillator structure is proposed. A SIW cavity with a high Q factor is employed as a frequency-selective tank to enhance the oscillator’s frequency stability. An antenna slot is integrated into the cavity, enabling efficient radiation while maintaining a compact form factor. The detailed design methodology and performance evaluation of the proposed structure are presented in Section 2, and the measurement validations are provided in Section 3.

2. SLOT-ANTENNA CAVITY-OSCILLATOR DESIGN

In this work, a compact system integrating antenna, oscillator, and coupling functionalities within a single circuit is developed to enhance performance and minimize footprint. This unified approach combines the radiating and resonating elements within the same physical structure. The main design challenge lies in achieving the necessary oscillation conditions — particularly the coupling coefficient — without degrading the antenna’s radiation performance, and vice-versa. A target frequency of 10 GHz was selected to align with related studies in the literature and to facilitate harmonic control and suppression of higher-order modes. This frequency also enables experimental validation using laboratory equipment that is readily available and well-suited for this band. To minimize dielectric and conductor losses, the Rogers 6002 substrate was chosen for its low-loss characteristics and proven suitability for high-frequency applications.

2.1. Cavity Design

As illustrated in Figure 1, the conventional three-port configuration is replaced with a compact two-port design. The TE_{210} mode is excited by introducing a microstrip inset near the center of the cavity, with the cavity dimensions defining the op-

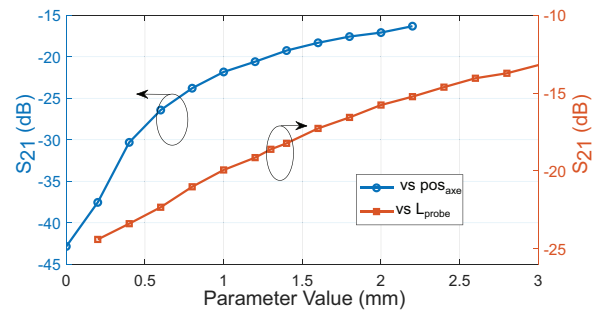


FIGURE 2. Parametric study results showing the variation of S_{21} with respect to the displacement parameter pos_{axe} and the probe length L_{probe} .

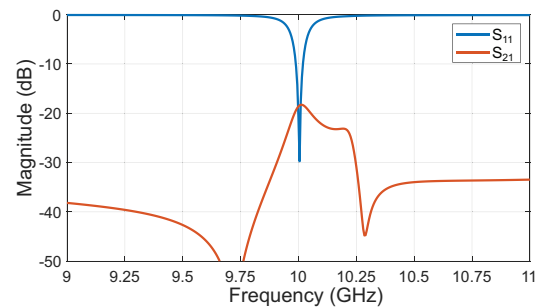


FIGURE 3. Coupling coefficient S_{21} versus frequency. Parameters: $L_{cavity} = 0.63$ mm, $W_{cavity} = 0.79$ mm, $L_{probe} = 0.22$ mm, $L_s = 0.02$ mm, $W_s = 0.25$ mm, $pos_{axe} = 0.01$ mm.

erating frequency to ensure resonance alignment with the slot. A perpendicular coupling probe is inserted to control the coupling, where its position and insertion depth serve as tunable parameters. Employing TE_{210} mode instead of the conventional TE_{110} mode reduces the loading effect of the coupling probe on the antenna. The feedback power coupled from the second port is governed by its location and insertion depth within the node region.

Figure 2 presents a parametric study of the two-port oscillator’s cavity. The probe insertion length L_{probe} affects the coupling, exhibiting a nearly linear behavior with S_{21} ranging between 12 and 25 dB. Similarly, the displacement parameter pos_{pos} influences the coupling strength, reaching a minimum at the symmetrical point. These results underscore the importance of precise geometrical tuning to optimize oscillator performance. The coupling coefficient S_{21} , optimized around 20 dB as a function of frequency, is shown in Figure 3. The resonance occurs at 10 GHz, with a -3 dB bandwidth of approximately 0.1 GHz, yielding to a quality factor of about 250. This high Q confirms the structure’s narrowband nature and excellent frequency selectivity. Moreover, the TE_{210} mode exhibits a higher conductor-limited quality factor Q_c than the fundamental TE_{110} mode, due to reduced surface current concentration and more favorable field distribution near the cavity walls [15].

Figure 4 shows the electric field 4(a), magnetic field 4(b), and surface current 4(c) distributions at the operating frequency of 10 GHz. The TE_{210} mode exhibits strong field confinement and symmetry around the central axis, and the surface current is

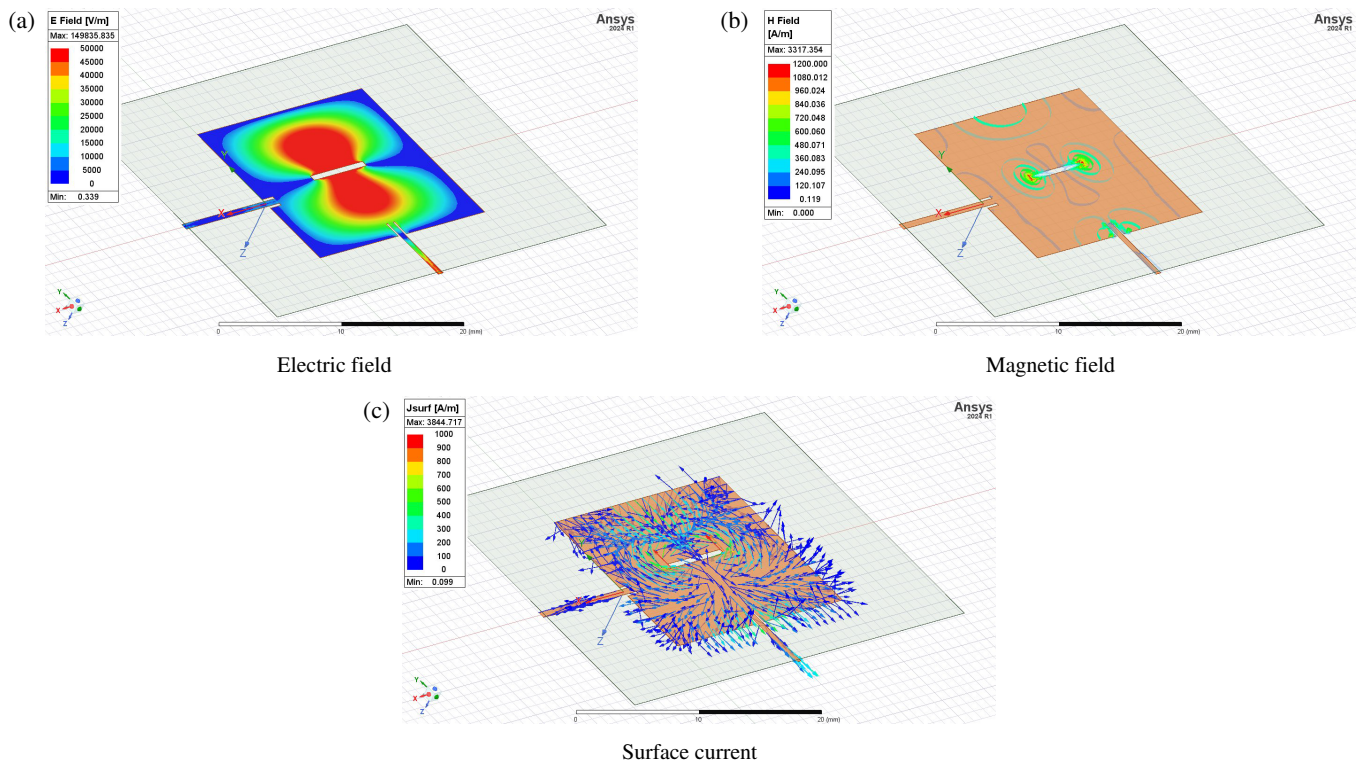


FIGURE 4. (a) Simulated electric field, (b) magnetic field, and (c) surface current distributions at the operating frequency of 10 GHz, highlighting the mode shape and confinement around the resonator structure.

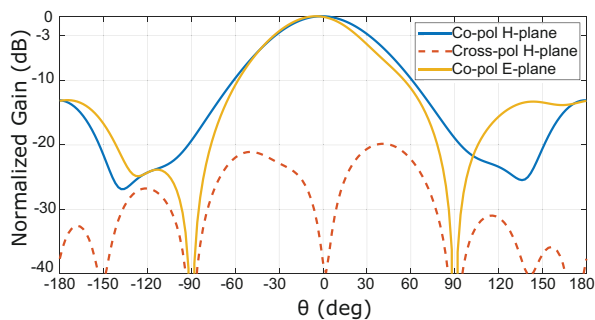


FIGURE 5. Normalized radiation patterns at 10 GHz for H -plane ($\Phi = 0^\circ$) and E -plane ($\Phi = 90^\circ$) cuts, showing co-polarization and cross-polarization components.

concentrated around the slot. Positioning the second port near a field node minimizes perturbation, enabling stable two-port operation without significantly degrading the mode shape. After validating the two-port cavity structure, a slot was integrated at the field node to avoid disturbing the cavity mode. The slot was designed to radiate at the same frequency as the oscillator. Integration of the slot introduces radiation loss, typically modeled as a resistive element, and slightly reduces the factor Q . Figure 5 presents the radiation patterns at 10 GHz. The main beam exhibits a co-polarized gain normalized to 0 dB, while the cross-polarization remains below -40 dB broadside, indicating excellent polarization purity. The Half-Power Beam-Width (HPBW) is approximately 60° in the H -plane and slightly narrower in the E -plane, with an achieved gain of approximately 7 dBi. The Front-to-Back Ratio (FBR) exceeds 20 dB, confirming the antenna's directional performance.

2.2. Oscillator Design

The feedback oscillator was designed using a linear circuit simulator following a systematic methodology. The process began with a full-wave electromagnetic simulation of the SIW cavity using High Frequency Structure Simulator (HFSS), from which S -parameters were extracted and imported into Advanced Design System (ADS). This allowed accurate integration of the cavity response into the oscillator loop. An HMC963LC4 low-noise amplifier was selected for its appropriate gain and noise figure characteristics. The amplifier was then combined with the SIW cavity to form the core of the feedback oscillator. The loop length was carefully adjusted to satisfy the phase condition for oscillation, ensuring a total phase shift of an integer multiple of 360° . As recommended in [8], the design targeted a loop gain of slightly more than 1 dB to account for gain compression when the amplifier operates in saturation. Minimizing the loop length required to meet the phase condition reduces reactive losses and improves phase noise performance, leading to faster startup.

After constructing the circuit, loop gain and phase measurements were performed to finalize tuning, as outlined in [8]. This step ensures that both the amplitude and phase conditions for sustained oscillation are satisfied, enabling stable operation of the active oscillator.

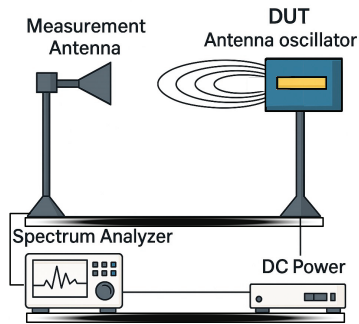
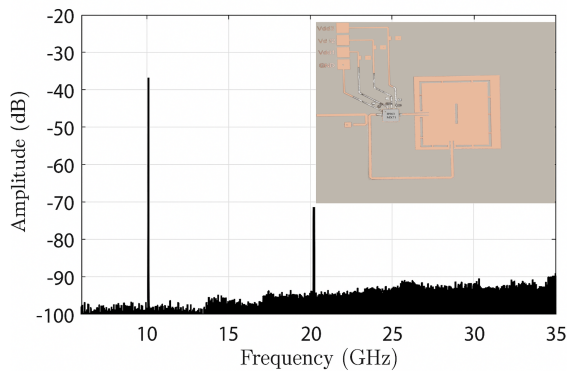
3. EXPERIMENTAL VALIDATION

As illustrated in Figure 6, an Over-The-Air (OTA) measurement setup has been used, where the proposed oscillator/antenna operates as the transmitter, and standardized

TABLE 1. Comparison of active integrated antenna oscillators from various works.

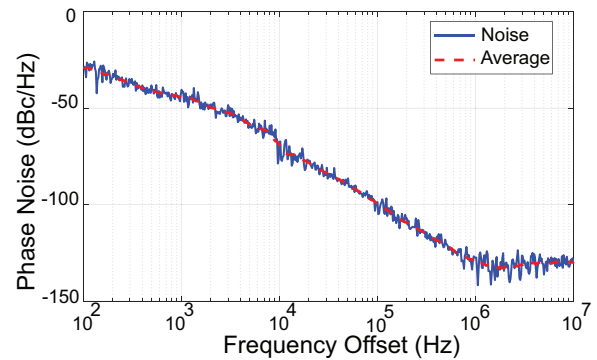
Parameter	[4]	[6]	[8]	[11]	This Work
Frequency of Operation (GHz)	7.97/8.9	11.87–12.36	0.927	7.13	10
Phase Noise (dBc/Hz)	−90 @ 100 kHz	−107 @ 1 MHz	−120 @ 100 MHz	−101.7 @ 100 kHz	−131 @ 1 MHz
Antenna Gain, Gt (dBi)	4.8/5.1	~ 5.5 (sim.)	3.2	N/A	6
Oscillator Type	-Feedback (x2)	-Feedback	-Feedback	Cross-Coupled	+Feedback
Q Factor	~15	N/A	250 (CRLH)	N/A	250
Circuit/Antenna Type	SDA ¹ (SIW)	SIW Patch	CPAIA ²	CCAA ³	SIW Slot Antenna
Size (λ_0)	3.01	0.22	0.36	4	4.3 ⁴

¹Self-diplexing antenna (SDA). ²Circularly polarized active integrated antenna (CPAIA). ³Cross-Coupled Active Antenna (CCAA) ⁴ Works in the 2nd mode.

**FIGURE 6.** Measurement setup.**FIGURE 7.** Analyzed spectrum with fabricated circuit under test.

antennas connected to a signal analyzer are positioned on the receiving side. Using the Keysight UXA signal analyzer N9040B, as shown in Figure 7, the oscillator output was characterized over a frequency range of 5 GHz to 35 GHz with a resolution bandwidth of 100.0 Hz.

The power spectrum is dominated by the fundamental tone, while higher-order harmonics are significantly attenuated — down to -35 dBc for the second harmonic and effectively suppressed for the third, thanks to the filtering effect of the cavity — oscillator configuration. The estimated output power at the fundamental frequency is approximately 0 dBm. Based on a measured received power of -37 dBm at a distance of 1 meter using a receiving antenna with a gain of 6 dBi, the transmitting system (oscillator + antenna) is effectively radiating an Equivalent Isotropic Radiated Power (EIRP) of approximately 9.4 dBm at 10 GHz.

**FIGURE 8.** Measured phase noise of the oscillator.

As shown in Figure 8, the phase noise performance of the proposed oscillator was evaluated using the Keysight signal analyzer. The measurement was conducted over a frequency offset range from 100 Hz to 10 MHz. At a 100 Hz offset, the oscillator exhibits a phase noise level of approximately -45 dBc/Hz, which decreases to around -125 dBc/Hz at a 1 MHz offset and further approaches -130 dBc/Hz at 10 MHz. This characteristic phase noise profile drops by approximately 20–30 dB per frequency. The low phase noise across a wide offset range confirms the oscillator's spectral purity and stability, making it suitable for high-frequency communication systems where low jitter and clean spectral behavior are critical.

To better highlight the performance and integration advantages of the proposed design, Table 1 provides a comparative overview of experimental results of several fixed-frequency antenna oscillator structures reported in the literature. The comparison includes key performance indicators, such as oscillation frequency, external quality factor, phase noise, radiated power or EIRP, physical footprint, and integration features. While prior works demonstrated various strengths — such as dual-band operation, harmonic suppression, and filtering integration — most relied on separate radiation and feedback paths or required additional components for stability. In contrast, the proposed structure uniquely integrates the oscillator and slot antenna within a single SIW cavity, offering a compact footprint, effective harmonic rejection, and low phase noise performance enabled by the high- Q TE_{210} mode and optimized feedback coupling.

4. CONCLUSION

This letter validates the architectural feasibility of an integrated antenna-oscillator utilizing an SIW cavity, where the frequency resonator (tank) and radiating slot element are co-designed on a single dielectric layer. The oscillator operates at 10 GHz, with frequency stability ensured by the high Q factor of the cavity, measured at 250. The oscillator also exhibits low phase noise of -131 dBc/Hz, while the slot antenna achieves a gain of 6 dBi also at the same frequency of 10 GHz. The proposed integration of the oscillator and antenna within a single structure enhances RF front-end integration, reduces size and loss, simplifies system architecture, and enables direct radiation of the oscillating signal. This approach is particularly well-suited for compact wireless systems such as internet of things (IoT) nodes, millimeter-wave sensors, and future 5G/6G transceivers.

REFERENCES

- [1] Cassivi, Y. and K. Wu, "Low cost microwave oscillator using substrate integrated waveguide cavity," *IEEE Microwave and Wireless Components Letters*, Vol. 13, No. 2, 48–50, 2003.
- [2] Yang, X.-L., X.-W. Zhu, and X. Wang, "An X-band low phase noise parallel-feedback oscillator based on SIW dual-mode filtering power divider," *IEEE Transactions on Circuits and Systems II: Express Briefs*, Vol. 71, No. 1, 61–65, 2024.
- [3] Bayderkhani, R., K. Forooraghi, and B. Abbasi-Arand, "Gain-enhanced SIW cavity-backed slot antenna with arbitrary levels of inclined polarization," *IEEE Antennas and Wireless Propagation Letters*, Vol. 14, 931–934, 2015.
- [4] Adhikary, M., S. K. Sahoo, A. Biswas, and M. J. Akhtar, "SIW-based self-oscillating concurrent dual-frequency active integrated antenna," *IEEE Antennas and Wireless Propagation Letters*, Vol. 18, No. 9, 1897–1901, 2019.
- [5] Wang, X. and W. Wu, "Design of low phase noise oscillator based on SIW multifunctional filtering device," *IEEE Transactions on Circuits and Systems II: Express Briefs*, Vol. 70, No. 1, 31–35, 2023.
- [6] Giuppi, F., A. Georgiadis, A. Collado, and M. Bozzi, "A compact, single-layer substrate integrated waveguide (SIW) cavity-backed active antenna oscillator," *IEEE Antennas and Wireless Propagation Letters*, Vol. 11, 431–433, 2012.
- [7] Nandi, S. and A. Mohan, "An SIW cavity-backed self-diplexing antenna," *IEEE Antennas and Wireless Propagation Letters*, Vol. 16, 2708–2711, 2017.
- [8] Djerafi, T., K. Wu, and D. Deslandes, "Temperature drift compensation technique for substrate integrated waveguide oscillator," *IEEE Microwave and Wireless Components Letters*, Vol. 22, No. 9, 489–491, 2012.
- [9] Huang, G.-C. and T.-G. Ma, "High-EIRP self-oscillating circularly polarized active integrated crossed-slot antenna," *IEEE Antennas and Wireless Propagation Letters*, Vol. 23, No. 1, 54–58, Jan. 2024.
- [10] Du, Z.-X., M. Cui, Y. Zhang, and C. Guo, "Miniaturized wide-band self-oscillating active integrated antenna with power enhancement," *IEEE Antennas and Wireless Propagation Letters*, Vol. 23, No. 10, 2964–2968, 2024.
- [11] Liu, Z.-H., H. N. Chu, and T.-G. Ma, "Self-oscillating active integrated antenna with harmonic suppression using metamaterial resonators and ground radiation," *IEEE Antennas and Wireless Propagation Letters*, Vol. 17, No. 9, 1687–1691, Sep. 2018.
- [12] Amiri, M., N. Masoumi, and M. Shahabadi, "Low phase-noise self-oscillating cross-coupled active antenna," *IEEE Transactions on Antennas and Propagation*, Vol. 66, No. 9, 4516–4523, Sep. 2018.
- [13] Du, Z.-X., H.-T. Zhou, J. Liu, and C. Guo, "Compact self-oscillating active integrated loop antenna with concurrent dual-band operation," *IEEE Antennas and Wireless Propagation Letters*, Vol. 23, No. 3, 1070–1074, Mar. 2024.
- [14] Rubiola, E., *Phase Noise and Frequency Stability in Oscillators*, Cambridge University Press, 2008.
- [15] Pozar, D. M., *Microwave Engineering*, 4th ed., John Wiley & Sons, 2012.
- [16] Razavi, B., *RF Microelectronics*, 2nd ed., Prentice Hall, 2012.